Iranian Journal of Numerical Analysis and Optimization
Vol. 14, No. 4, 2024, pp 1224–1246
https://doi.org/10.22067/ijnao.2024.87501.1419
https://ijnao.um.ac.ir/

Research Article

An efficient collocation scheme for new type of variable-order fractional Lane–Emden equation

H. Azin*, A. Habibirad, E. Hesameddini, M.H. Heydari

Abstract

The fractional Lane–Emden model illustrates different phenomena in astrophysics and mathematical physics. This paper involves the Vieta–Lucas ($\mathcal{V}t$-$\mathcal{L}$) bases to solve types of variable-order ($\mathcal{V}$-$\mathcal{O}$) fractional Lane–Emden

*Corresponding author

Received ; revised ; accepted

Hadis Azin
Department of Mathematics and Computer Sciences, Hakim Sabzevari University, Sabzevar, Iran. e-mail: h.azin1370@gmail.com

Ali Habibirad
Department of Mathematics and Computer Sciences, Hakim Sabzevari University, Sabzevar, Iran. e-mail: a.habibirad@sutech.ac.ir

Esmail Hesameddini
Department of Mathematics, Shiraz University of Technology, Shiraz, Iran. e-mail: hesameddini@sutech.ac.ir

Mohammad Hossein Heydari
Department of Mathematics, Shiraz University of Technology, Shiraz, Iran. e-mail: heydari@sutech.ac.ir

How to cite this article
Azin, H., Habibirad, A., Hesameddini, E. and Heydari, M.H., An efficient collocation scheme for new type of variable-order fractional Lane–Emden equation. *Iran. J. Numer. Anal. Optim.*, 2024; 14(4): 1224-1246. https://doi.org/10.22067/ijnao.2024.87501.1419

equation (linear and nonlinear). The operational matrix of the $\mathcal{V}$-$\mathcal{O}$ fractional derivative is obtained for the $\mathcal{V}t$-$\mathcal{L}$ polynomials. In the established approach, these polynomials are applied to transform the main problem into an algebraic equations system. To indicate the performance and capability of the scheme, a number of examples are presented for various types of $\mathcal{V}$-$\mathcal{O}$ fractional Lane–Emden equations. Also, for one example, a comparison is done between the calculated results by our technique and those obtained via the Bernoulli polynomials. Overall, this paper introduces a new methodology for solving $\mathcal{V}$-$\mathcal{O}$ fractional Lane–Emden equations using $\mathcal{V}t$-$\mathcal{L}$ bases. The derived operational matrix and the transformation to an algebraic equation system offer practical advantages in solving these equations efficiently. The presented examples and comparative analysis highlight the effectiveness and validity of the proposed technique, contributing to the understanding and advancement of fractional Lane–Emden models in astrophysics and mathematical physics.

AMS subject classifications (2020): 34A08; 65L60; 65N35; 35L10

Keywords: Lane–Emden equation; Vieta–Lucas polynomials; Variable-order fractional differential equation.

1 Introduction

Due to the helpful usage of fractional calculus in many scientific and engineering fields [7, 12, 25], from the first decade of this century until now, this issue has been challenging for researchers and will certainly continue in the coming decades. Finding the explicit solution for these equations is difficult and sometimes impossible. Therefore, many numerical techniques are extended for solving fractional differential equations. For example, interested readers can refer to [3, 17, 13, 22, 36, 35] and references therein.

Variable-order ($\mathcal{V}$-$\mathcal{O}$) operators are a natural generalization of operators with constant fractional order. In these types of operators, orders can be considered as a function of time, space, or both. In 1993, the first definition for this class of equations was provided by Samko and Ross [34]. Many dynamic procedures may vary by time or place. The fractional order role in these procedures shows that $\mathcal{V}$calculus is the normal prospect for supplying a useful

mathematical plan to explain complicated dynamical models. For example, $\mathcal{V}$-$\mathcal{O}$ fractional derivatives have been used for the processing of geographical data in [9], diffusion in [38], signature verification in [40], and viscoelasticity in [8]. Several mapping effects on the fractional operators in types of cases in Hölder spaces expanded for the topic of $\mathcal{V}$-$\mathcal{O}$ in [32]. Researchers have done many studies on the numerical approaches for solving the $\mathcal{V}$-$\mathcal{O}$ fractional problems. For example in [24], the $\mathcal{V}$-$\mathcal{O}$ diffusion equation is discussed with the conditionally stable explicit finite difference method. Zhuang et al. [44] considered conditionally stable explicit and unconditionally stable implicit methods in the $\mathcal{V}$-$\mathcal{O}$ fractional advection-diffusion equation. The scholars of [13] introduced a meshless moving Kriging interpolation scheme to solve the two-dimensional $\mathcal{V}$-$\mathcal{O}$ fractional mobile/immobile advection-diffusion problem. The Adams–Bashforth–Moulton predictor-corrector technique was proposed in [39, 26] to simulate $\mathcal{V}$-$\mathcal{O}$ fractional differential equations with time delays. To see other properties and numerical schemes regarding $\mathcal{V}$-$\mathcal{O}$ fractional differential equations, see [29] and references therein.

The Lane–Emden equations play a significant role in the fields of engineering sciences and physics. These equations find wide application in addressing various phenomena across disciplines such as thermodynamics, fluid mechanics, mathematical physics, and astrophysics. Notable examples include modeling stellar structures, analyzing isothermal gas spheres, studying thermionic currents, and investigating the thermal behavior of spherical gas clouds [10, 5, 11, 6].

Various methods have been employed to tackle Lane–Emden problems effectively, including the Homotopy technique [41], the B-Spline approach [4], the modified variational method [37], Lie group analysis [21], the Adomian and modified Adomian decomposition techniques [42, 23], finite element techniques [18], transform differential procedures [43], Taylor's series method [14], the Legendre wavelets method [20], and the rational Bernoulli collocation approach [28]. For a more in-depth exploration of Lane–Emden equations, encompassing their variations, historical context, and practical applications, interested individuals are encouraged to consult the work [1] and its associated references.

In this study, consider the $\mathcal{V}$-$\mathcal{O}$ fractional Lane–Emden model as

$$ {}_0^cD_{\mathfrak{t}}^{\varrho(\mathfrak{t})}\nu(\mathfrak{t}) + \frac{\xi}{\mathfrak{t}^{\varrho(\mathfrak{t})-\varsigma(\mathfrak{t})}}\,{}_0^cD_{\mathfrak{t}}^{\varsigma(\mathfrak{t})}\nu(\mathfrak{t}) + F(\mathfrak{t},\nu(\mathfrak{t})) = g(\mathfrak{t}), \qquad 0 \le \mathfrak{t} \le 1, \tag{1} $$

subject to the initial conditions

$$ \begin{cases} \nu(0) = \nu_0, \\ \nu'(0) = \nu_1, \end{cases} \tag{2} $$

where $1 < \varrho(\mathfrak{t}) < 2$, $0 < \varsigma(\mathfrak{t}) < 1$. Also, ξ is a positive constant, $F(\mathfrak{t},\nu(\mathfrak{t}))$, and $g(\mathfrak{t})$ are given continuous functions. The approximate solution of the classical fractional order of this equation has been investigated by Bernoulli polynomials in [33]. In this work, we use the $\mathcal{V}t$-$\mathcal{L}$ polynomials to solve the above form of this equation. The $\mathcal{V}t$-$\mathcal{L}$ polynomials were introduced for the first time in the year 2020 and used to solve fractional advection-dispersion equations [2]. Also, the uniform convergence and error bound of the $\mathcal{V}t$-$\mathcal{L}$ polynomials has been checked in [2]. Despite the accuracy of these polynomials in approximating functions, they have not been used in constructing numerical methods for solving various problems. In [27], a numerical method was presented with the operational matrix of $\mathcal{V}t$-$\mathcal{L}$ polynomials to solve the fractional Bagley–Torvik equation, initial value problems, and nonhomogenous multi-order fractional problems. Researchers in [19] used these polynomials to calculate the approximate solution of the multi-Pantograph delay problems with singularity and compare the computed results with the exact one. The capability and performance of the numerical scheme established upon the $\mathcal{V}t$-$\mathcal{L}$ polynomials to solve the coupled nonlinear $\mathcal{V}$-$\mathcal{O}$ fractional Ginzburg-Landau equations [15] encouraged us to use these polynomials to solve the $\mathcal{V}$-$\mathcal{O}$ fractional Lane–Emden problem. For this purpose, we compute the $\mathcal{V}$-$\mathcal{O}$ fractional derivative and the classical derivative operational matrices of the $\mathcal{V}t$-$\mathcal{L}$ polynomials. The solution $\nu(\mathfrak{t})$ is expanded in terms of these basis polynomials, and the linear/nonlinear equation is converted to the linear/ nonlinear algebraic equation system. The capability of the proposed scheme is obtained through several examples.

Numerical methods based on operational matrices have proven to be highly effective in solving mathematical problems, particularly those involving differential and integral equations. Unlike traditional methods that directly calculate derivatives and integrals, the operational matrix method uti-

lizes the operational matrices of derivatives and integrals. This approach offers several advantages, such as reducing CPU time due to the sparsity of the matrices and the presence of zero elements.

The operational matrix method is a powerful numerical technique for solving differential equations due to its simplicity, efficiency, accuracy, versatility, flexibility, and numerical stability. However, it is important to be aware of its limitations, including discretization errors, limited applicability to complex geometries, computational requirements, convergence issues, and limited support for discontinuous solutions. By considering these factors, researchers and practitioners can employ the operational matrix method effectively and make informed decisions regarding its application in various scientific and engineering fields.

The outline of the work is as follows: Several characteristics and concepts about $\mathcal{V}$-$\mathcal{O}$ fractional derivative in Caputo form are mentioned in section 2. The $\mathcal{V}t$-$\mathcal{L}$ polynomials are introduced in section 3. The formulation of the presented approach is explained in section 4. Several examples of linear and nonlinear types of the problem under study are examined in section 5. The conclusion of this work is briefly expressed in section 6.

2 $\mathcal{V}$-$\mathcal{O}$ fractional calculus

In this part, we introduce the indispensable relations and definitions of $\mathcal{V}$-$\mathcal{O}$ fractional calculus, which are required in our work.

Definition 1. [30] Let μ and $\zeta > 0$. The generalized Mittag-Leffler function is as follows:

$$\mathbf{E}_{\mu,\zeta}(\mathfrak{t}) = \sum_{i=0}^{\infty} \frac{\mathfrak{t}^i}{\Gamma(\mu i + \zeta)}, \tag{3}$$

where $\mathfrak{t} \in \mathbb{C}$.

Definition 2. [16] For a continuous function $\theta : \mathbb{R}^+ \cup \{0\} \longrightarrow (\hat{n}-1, \hat{n}]$ with $\hat{n} \in \mathbb{N}$, the $\mathcal{V}$-$\mathcal{O}$ fractional derivative of the function $\nu(\mathfrak{t})$ in the Caputo form is determined as

$$ {}_0^c D_{\mathfrak{t}}^{\theta(\mathfrak{t})}\nu(\mathfrak{t}) = \begin{cases} \dfrac{1}{\Gamma(\hat{n}-\theta(\mathfrak{t}))}\displaystyle\int_0^{\mathfrak{t}} (\mathfrak{t}-\rho)^{\hat{n}-\theta(\mathfrak{t})-1}\frac{d^{\hat{n}}\nu(\rho)}{d\rho^{\hat{n}}}d\rho, & \theta(\mathfrak{t}) \in (\hat{n}-1,\hat{n}), \\ \dfrac{d^{\hat{n}}\nu(\mathfrak{t})}{d\mathfrak{t}^{\hat{n}}}, & \theta(\mathfrak{t}) = \hat{n}. \end{cases} \tag{4} $$

Lemma 1. Let the assumptions of the above definition be satisfied. Then, we have

$$ {}_0^c D_{\mathfrak{t}}^{\theta(\mathfrak{t})}\mathfrak{t}^{\mathbf{k}} = \begin{cases} 0, & \mathbf{k} = 0,1,\ldots,\hat{n}-1, \\ \dfrac{\Gamma(\mathbf{k}+1)}{\Gamma(\mathbf{k}+1-\theta(\mathfrak{t}))}\mathfrak{t}^{\mathbf{k}-\theta(\mathfrak{t})}, & \mathbf{k} \geq \hat{n}. \end{cases} \tag{5} $$

3 The $\mathcal{V}t$-$\mathcal{L}$ polynomials

This section is dedicated to introduce the $\mathcal{V}t$-$\mathcal{L}$ polynomials and some of their properties.

Definition 3. [31, 15] The $\mathcal{V}t$-$\mathcal{L}$ polynomials are defined over $[0,1]$ as

$$ \mathcal{V}_j^*(\mathfrak{t}) = \begin{cases} 2, & j = 0, \\ \displaystyle\sum_{l=0}^{j}(-1)^{j-l}\frac{2^{2l+1}j(j+l-1)!}{(2l)!(j-l)!}\mathfrak{t}^l, & j \geq 1. \end{cases} \tag{6} $$

The orthogonal property of these polynomials is satisfied, which means that

$$ \int_0^1 \mathcal{V}_j^*(\mathfrak{t})\mathcal{V}_{\hat{j}}^*(\mathfrak{t})\varpi(\mathfrak{t})d\mathfrak{t} = \begin{cases} 4\pi, & j = \hat{j} = 0, \\ 2\pi, & j = \hat{j} \neq 0, \\ 0, & j \neq \hat{j}, \end{cases} \tag{7} $$

where $\varpi(\mathfrak{t}) = \dfrac{1}{\sqrt{\mathfrak{t}-\mathfrak{t}^2}}$. Any function $\nu(\mathfrak{t}) \in L^2_{\varpi}[0,1]$ can be expanded with the $\mathcal{V}t$-$\mathcal{L}$ polynomials as

$$ \nu(\mathfrak{t}) \simeq \nu_N(\mathfrak{t}) = \sum_{j=0}^{N} c_j\mathcal{V}_j^*(\mathfrak{t}) \triangleq \mathbf{C}^T\Upsilon(\mathfrak{t}), \tag{8} $$

where

$$ \begin{aligned} \mathbf{C} &= [\hat{c}_0 \quad \hat{c}_1 \quad \cdots \quad \hat{c}_N]^T, \\ \Upsilon(\mathfrak{t}) &= [\mathcal{V}_0^*(\mathfrak{t}) \quad \mathcal{V}_1^*(\mathfrak{t}) \quad \cdots \quad \mathcal{V}_N^*(\mathfrak{t})]^T, \end{aligned} \tag{9} $$

and

$$\hat{c}_j = \frac{1}{\lambda_j}\int_0^1 \nu(\mathfrak{t})\mathcal{V}_j^*(\mathfrak{t})\varpi(\mathfrak{t})d\mathfrak{t}, \qquad j = 0, 1, \ldots, N, \tag{10}$$

with

$$\lambda_j = \int_0^1 \left(\mathcal{V}_j^*(\mathfrak{t})\right)^2 \varpi(\mathfrak{t})d\mathfrak{t} = \begin{cases} 4\pi, & j = 0, \\ 2\pi, & j = 1, 2, \ldots, N. \end{cases} \tag{11}$$

The following theorem demonstrates the uniform convergence of the $\mathcal{V}t$-$\mathcal{L}$ polynomials and its error bound for approximating the function $\nu(\mathfrak{t})$.

Theorem 1. [2] Assume that $\nu(\mathfrak{t}) \in L^2_\varpi$ with $\varpi(\mathfrak{t})$ and $|\nu''(\mathfrak{t})| < K$ such that K is a positive constant. Then, $\nu_N(\mathfrak{t}) \longrightarrow \nu(\mathfrak{t})$ as $N \longrightarrow \infty$. Moreover, the coefficients in relation (8) satisfy

$$|\hat{c}_j| \leq \frac{K}{4j(j^2-1)}, \qquad j > 2. \tag{12}$$

Also, the error bound will be obtained as

$$\|\nu(\mathfrak{t}) - \nu_N(\mathfrak{t})\|_{L^2_\varpi} < \frac{K}{12N^{\frac{3}{2}}}. \tag{13}$$

In the next theorem, the ordinary derivative matrix and the $\mathcal{V}$-$\mathcal{O}$ fractional of the $\mathcal{V}t$-$\mathcal{L}$ polynomials are derived.

Theorem 2. The differentiation of the vector $\Upsilon(\mathfrak{t})$ in (9) satisfies the following relation

$$\frac{d\Upsilon(\mathfrak{t})}{d\mathfrak{t}} \simeq \mathcal{D}^{(1)}\Upsilon(\mathfrak{t}), \tag{14}$$

in which $\mathcal{D}^{(1)}$ is an $(N+1)\times(N+1)$ matrix which its entries is computed by

$$[\mathcal{D}^{(1)}]_{ij} = \begin{cases} 0, & i = 1, \\ \varphi_{ij}, & i = 2, 3, \ldots, N+1, \end{cases} \tag{15}$$

in which

$$\varphi_{ij}=\begin{cases}\dfrac{1}{4\pi}\displaystyle\sum_{l=1}^{i-1}(-1)^{i-l-1}\frac{2^{2(l+1)}(i-1)(i+l-2)!l}{(2l)!(i-l-1)!}\frac{\sqrt{\pi}\Gamma(l-\frac{1}{2})}{\Gamma(l)}, \\ \qquad\qquad\qquad\qquad\qquad\qquad\qquad\qquad\qquad\qquad j=1, \\ \dfrac{1}{2\pi}\displaystyle\sum_{l=1}^{i-1}\sum_{s=0}^{j-1}(-1)^{i+j-l-s-2}\left(\frac{2^{2(l+s+1)}(i-1)(j-1)(i+l-2)!(j+s-2)!l}{(2l)!(2s)!(i-l-1)!(j-s-1)!}\right. \\ \qquad\qquad\left.\frac{\sqrt{\pi}\Gamma(l+s-\frac{1}{2})}{\Gamma(l+s)}\right), \\ \qquad\qquad\qquad\qquad\qquad\qquad\qquad\qquad\qquad\qquad j=2,3,\ldots,N+1.\end{cases}\tag{16}$$

Proof. For $\hat{i}=0$, the proof is obvious. For $\hat{i}=1,\ldots,N$ from (6), we get

$$\frac{\mathcal{V}_{\hat{i}}^{*}(\mathfrak{t})}{d\mathfrak{t}}=\sum_{l=1}^{\hat{i}}(-1)^{\hat{i}-l}\frac{2^{2l+1}\hat{i}(\hat{i}+l-1)!l}{(2l)!(\hat{i}-l)!}\mathfrak{t}^{l-1}.\tag{17}$$

Approximating the above relation with the $\mathcal{V}t$-$\mathcal{L}$ polynomials results in

$$\frac{\mathcal{V}_{\hat{i}}^{*}(\mathfrak{t})}{d\mathfrak{t}}\simeq\sum_{\hat{j}=0}^{N}\mathcal{D}_{\hat{i}\hat{j}}^{(1)}\mathcal{V}_{\hat{j}}^{*}(\mathfrak{t}),\qquad\hat{i}=1,2,\ldots,N,\tag{18}$$

in which, for $\hat{j}=0$, one obtains

$$\begin{aligned}\mathcal{D}_{10}^{(1)}&=\frac{1}{\lambda_0}\int_0^1\frac{\mathcal{V}_{\hat{i}}^{*}(\mathfrak{t})}{d\mathfrak{t}}\mathcal{V}_0^{*}(\mathfrak{t})\varpi(\mathfrak{t})d\mathfrak{t}\\&=\frac{1}{4\pi}\sum_{l=1}^{\hat{i}}(-1)^{i-l}\frac{2^{2l+1}\hat{i}(\hat{i}+l-1)!l}{(2l)!(\hat{i}-l)!}\int_0^1\frac{2\mathfrak{t}^{l-1}}{\sqrt{\mathfrak{t}-\mathfrak{t}^2}}d\mathfrak{t}\\&=\frac{1}{4\pi}\sum_{l=1}^{\hat{i}}(-1)^{\hat{i}-l}\frac{2^{2(l+1)}\hat{i}(\hat{i}+l-1)!l}{(2l)!(\hat{i}-l)!}\frac{\sqrt{\pi}\Gamma(l-\frac{1}{2})}{\Gamma(l)},\end{aligned}\tag{19}$$

and for $\hat{j}=1,2,\ldots,N$,

$$\begin{aligned}\mathcal{D}_{\hat{i}\hat{j}}^{(1)}&=\frac{1}{\lambda_j}\int_0^1\frac{\mathcal{V}_{\hat{i}}^{*}(\mathfrak{t})}{d\mathfrak{t}}\mathcal{V}_{\hat{j}}^{*}(\mathfrak{t})\varpi(\mathfrak{t})d\mathfrak{t}\\&=\frac{1}{2\pi}\sum_{l=1}^{\hat{i}}\sum_{s=0}^{\hat{j}}\left((-1)^{\hat{i}+\hat{j}-l-s}\frac{2^{2(l+s+1)}\hat{i}\hat{j}(\hat{i}+l-1)!(\hat{j}+s-1)!l}{(2l)!(2s)!(\hat{i}-l)!(\hat{j}-s)!}\right)\int_0^1\frac{\mathfrak{t}^{l+s-1}}{\sqrt{\mathfrak{t}-\mathfrak{t}^2}}d\mathfrak{t}\\&=\frac{1}{2\pi}\sum_{l=1}^{\hat{i}}\sum_{s=0}^{\hat{j}}\left((-1)^{\hat{i}+\hat{j}-l-s}\frac{2^{2(l+s+1)}\hat{i}\hat{j}(\hat{i}+l-1)!(\hat{j}+s-1)!l}{(2l)!(2s)!(\hat{i}-l)!(\hat{j}-s)!}\right)\frac{\sqrt{\pi}\Gamma(l+s-\frac{1}{2})}{\Gamma(k+s)}.\end{aligned}\tag{20}$$

Therefore, by replacing $\hat{i}=i-1$ and $\hat{j}=j-1$, the proof is completed. □

For example, for $N = 5$, one can get

$$\mathcal{D}^{(1)} = \begin{bmatrix} 0 & 0 & 0 & 0 & 0 & 0 \\ 2 & 0 & 0 & 0 & 0 & 0 \\ 0 & 8 & 0 & 0 & 0 & 0 \\ 6 & 0 & 12 & 0 & 0 & 0 \\ 0 & 16 & 0 & 16 & 0 & 0 \\ 10 & 0 & 20 & 0 & 20 & 0 \end{bmatrix}.$$

Lemma 2. The vector $\Upsilon(\mathfrak{t})$ in (9) can be rewritten by

$$\Upsilon(\mathfrak{t}) = \mathfrak{R}\dot{\mathbf{X}}, \tag{21}$$

where

$$\dot{\mathbf{X}} = [1 \quad \mathfrak{t} \quad \mathfrak{t}^2 \quad \cdots \quad \mathfrak{t}^n]^T, \tag{22}$$

and $\mathfrak{R}$ is an $(n+1)$ square upper triangular matrix and

$$[\mathfrak{R}]_{ij} = \begin{cases} 2, & i = j = 1, \\ \mathfrak{u}_{ij}, & j \le i, \end{cases} \tag{23}$$

in which

$$\mathfrak{u}_{ij} = \frac{(-1)^{i-j} 2^{2j+1} i(i+j-1)!}{(2j)!(i-j)!}. \tag{24}$$

Proof. By considering (6) and (9), one obtains

$$\begin{aligned} \Upsilon(\mathfrak{t}) &= [\mathcal{V}_0^*(\mathfrak{t}) \quad \mathcal{V}_1^*(\mathfrak{t}) \quad \mathcal{V}_2^*(\mathfrak{t}) \quad \cdots \quad \mathcal{V}_N^*(\mathfrak{t})]^T \\ &= [2 \quad \mathfrak{u}_{10} + \mathfrak{u}_{11}\mathfrak{t} \quad \mathfrak{u}_{20} + \mathfrak{u}_{21}\mathfrak{t} + \mathfrak{u}_{22}\mathfrak{t}^2 \quad \cdots \quad \mathfrak{u}_{n0} + \mathfrak{u}_{n1}\mathfrak{t} + \ldots + \mathfrak{u}_{nn}\mathfrak{t}^n]^T \\ &= \begin{bmatrix} 2 & 0 & 0 & 0 & \cdots & 0 \\ \mathfrak{u}_{10} & \mathfrak{u}_{11} & 0 & 0 & \cdots & 0 \\ \mathfrak{u}_{20} & \mathfrak{u}_{21} & \mathfrak{u}_{22} & 0 & \cdots & 0 \\ \vdots & \vdots & \vdots & \vdots & \vdots & \vdots \\ \mathfrak{u}_{n0} & \mathfrak{u}_{n1} & \mathfrak{u}_{n2} & \mathfrak{u}_{n3} & \cdots & \mathfrak{u}_{nn} \end{bmatrix} \begin{bmatrix} 1 \\ \mathfrak{t} \\ \mathfrak{t}^2 \\ \vdots \\ \mathfrak{t}^n \end{bmatrix}, \end{aligned} \tag{25}$$

in which $\mathfrak{u}_{ij}$ is defined in (24). □

Lemma 3. Let $\dot{\mathbf{X}}$ be the vector defined in (22). Also, let $\mathbf{q}-1<\sigma(\mathfrak{t})<\mathbf{q}$ be a continuous function given in $[0,1]$. Then, the $\mathcal{V}$-$\mathcal{O}$ fractional derivative of $\dot{\mathbf{X}}$ is obtained as

$$ {}_0^cD_{\mathfrak{t}}^{\sigma(\mathfrak{t})}\dot{\mathbf{X}}=\mathbf{Q}^{\sigma(\mathfrak{t})}\dot{\mathbf{X}}, \tag{26}$$

where $\mathbf{Q}^{\sigma(\mathfrak{t})}$ is the square $(n+1)$-matrix whose first $\mathbf{q}$ columns are zero and

$$\mathbf{Q}^{\sigma(\mathfrak{t})}=\begin{bmatrix} 0 & 0 & \cdots & 0 & 0 & \cdots & 0\\ 0 & 0 & \cdots & 0 & 0 & \cdots & 0\\ \vdots & \vdots & \ddots & \vdots & \vdots & \ddots & \vdots\\ 0 & 0 & \cdots & 0 & 0 & \cdots & 0\\ 0 & 0 & \cdots & \dfrac{\Gamma(\mathbf{q}+1)}{\Gamma(\mathbf{q}+1-\sigma(\mathfrak{t}))}\mathfrak{t}^{-\xi} & 0 & \cdots & 0\\ 0 & 0 & \cdots & 0 & \dfrac{\Gamma(\mathbf{q}+2)}{\Gamma(\mathbf{q}+2-\sigma(\mathfrak{t}))}\mathfrak{t}^{-\xi} & \cdots & 0\\ \vdots & \vdots & \ddots & \vdots & \vdots & \ddots & \vdots\\ 0 & 0 & \cdots & 0 & 0 & \cdots & \dfrac{\Gamma(n+1)}{\Gamma(n+1-\sigma(\mathfrak{t}))}\mathfrak{t}^{-\xi} \end{bmatrix}. \tag{27}$$

Proof. According to Lemma 1, the proof is obvious. □

Now, we compute the operational matrix of $\mathcal{V}$-$\mathcal{O}$ fractional derivative of the $\mathcal{V}t$-$\mathcal{L}$ polynomials.

Theorem 3. Let $\Upsilon(\mathfrak{t})$ be the $\mathcal{V}t$-$\mathcal{L}$ polynomials vector defined in (9) and let $\sigma(\mathfrak{t})$ be a function introduced in Lemma 3. Then, the $\mathcal{V}$-$\mathcal{O}$ fractional derivative of order $\sigma(\mathfrak{t})$ is computed as follows

$$ {}_0^cD_{\mathfrak{t}}^{\sigma(\mathfrak{t})}\Upsilon(\mathfrak{t})=\mathfrak{D}^{\sigma(\mathfrak{t})}\Upsilon(\mathfrak{t}), \tag{28}$$

where $\mathfrak{D}^{\sigma(\mathfrak{t})}=\mathfrak{R}\mathbf{Q}^{\sigma(\mathfrak{t})}\mathfrak{R}^{-1}$ is the matrix of $\sigma(\mathfrak{t})$ $\mathcal{V}$-$\mathcal{O}$ fractional derivative for the $\mathcal{V}t$-$\mathcal{L}$ polynomials.

Proof. Using Lemmas 2 and 3, one can get

$$\begin{aligned} {}_0^cD_{\mathfrak{t}}^{\sigma(\mathfrak{t})}\Upsilon(\mathfrak{t}) &= {}_0^cD_{\mathfrak{t}}^{\sigma(\mathfrak{t})}\left(\mathfrak{R}\dot{\mathbf{X}}\right)=\mathfrak{R}\,{}_0^cD_{\mathfrak{t}}^{\sigma(\mathfrak{t})}\dot{\mathbf{X}}\\ &=\mathfrak{R}\mathbf{Q}^{\sigma(\mathfrak{t})}\dot{\mathbf{X}}=\left(\mathfrak{R}\mathbf{Q}^{\sigma(\mathfrak{t})}\mathfrak{R}^{-1}\right)\Upsilon(\mathfrak{t})=\mathfrak{D}^{\sigma(\mathfrak{t})}\Upsilon(\mathfrak{t}), \end{aligned} \tag{29}$$

and the proof is performed. □

4 Description of the scheme

In this part, we state a spectral method via the $\mathcal{V}t$-$\mathcal{L}$ polynomials for the approximate solution of the $\mathcal{V}$-$\mathcal{O}$ fractional Lane–Emden equation expressed in (1). For this purpose, assume that

$$\nu(\mathfrak{t}) \simeq \nu_N(\mathfrak{t}) = \sum_{j=0}^{N} c_j \mathcal{V}_j^*(\mathfrak{t}) \triangleq \mathbf{C}^T \Upsilon(\mathfrak{t}), \tag{30}$$

where $\mathbf{C}$ is a vector with unknown elements and $\Upsilon(\mathfrak{t})$ is defined in relation (9). Using Theorem 3 implies that

$${}_0^c D_{\mathfrak{t}}^{\varrho(\mathfrak{t})} \nu(\mathfrak{t}) \simeq \mathbf{C}^T \mathfrak{D}^{\varrho(\mathfrak{t})} \Upsilon(\mathfrak{t}), \tag{31}$$

and

$${}_0^c D_{\mathfrak{t}}^{\varsigma(\mathfrak{t})} \nu(\mathfrak{t}) \simeq \mathbf{C}^T \mathfrak{D}^{\varsigma(\mathfrak{t})} \Upsilon(\mathfrak{t}). \tag{32}$$

Substituting (30)–(32) into (1) results in

$$\mathbf{C}^T \mathfrak{D}^{\varrho(\mathfrak{t})} \Upsilon(\mathfrak{t}) + \frac{\mu}{\mathfrak{t}^{\varrho(\mathfrak{t})-\varsigma(\mathfrak{t})}} \mathbf{C}^T \mathfrak{D}^{\varsigma(\mathfrak{t})} \Upsilon(\mathfrak{t}) + F(\mathfrak{t}, \mathbf{C}^T \Upsilon(\mathfrak{t})) - g(\mathfrak{t}) \triangleq \mathbf{R}(\mathfrak{t}). \tag{33}$$

Moreover, from (2), (30), and Theorem 2, we get

$$\begin{cases} \Lambda_0 \triangleq \mathbf{C}^T \Upsilon(0) - \nu_0 \simeq 0, \\ \Lambda_1 \triangleq \mathbf{C}^T \mathcal{D}^{(1)} \Upsilon(0) - \nu_1 \simeq 0. \end{cases} \tag{34}$$

Eventually, one obtains a numerical solution for (1) by solving relation (33) with initial conditions (34) in the collocation points $\mathfrak{t}_{\bar{i}} = \dfrac{2\bar{i}-1}{2(N+1)}$ with $\bar{i} = 1, 2, \ldots, N-1$, and through substituting in (30). The program of the proposed numerical method in pseudo-code format is designed in Algorithm 1. It is crucial to emphasize that the solution to the system of equations (33) and (34) is achieved by utilizing the "fsolve" command within the Maple 18 software.

Algorithm 1: The proposed method algorithm

Inputs: $N > 0$; $\varsigma(\mathfrak{t}) \in (0,1]$; $\varrho(\mathfrak{t}) \in (1,2]$; g; ν_0; ν_1.

Step 1: Define the functions $\mathcal{V}_j^*(\mathfrak{t})$ via (6).

Step 2: Construct the vector $\Upsilon(\mathfrak{t})$ and the matrix $\mathcal{D}^{(1)}$ by (9) and Theorem 2, respectively.

Step 3: Make of the matrices $\mathfrak{D}^{\varrho(\mathfrak{t})}$ and $\mathfrak{D}^{\varsigma(\mathfrak{t})}$ using Theorem (3).

Step 4: Construct the vector $\mathbf{C}$ in (30).

Step 5: Define $\mathbf{R}(\mathfrak{t})$, Λ_0, and Λ_1 in (33) and (34).

Step 6: Extract the algebraic system by the collocation points x_i.

Step 7: Solve the obtained system and compute the vector $\mathbf{C}$.

Outputs: The numerical solution $\nu_N(\mathfrak{t})$.

5 Numerical results

Here, four numerical examples are proposed to examine the accuracy of presented technique. To do this, we use the maximum absolute error as

$$L_\infty = \max_{0\le x\le 1} |\nu(\mathfrak{t}) - \nu_N(\mathfrak{t})|, \tag{35}$$

where $\nu(\mathfrak{t})$ and $\nu_N(\mathfrak{t})$ are the analytical and numerical solution with $\mathcal{V}t$-$\mathcal{L}$ polynomials, respectively. Also, the calculations are carried out by Maple 17 with 25 digits.

Example 1. For the first example, consider the problem

$$ {}_0^c D_{\mathfrak{t}}^{\varrho(\mathfrak{t})}\nu(\mathfrak{t}) + \frac{1}{\mathfrak{t}^{\varrho(\mathfrak{t})-\varsigma(\mathfrak{t})}}\, {}_0^c D_{\mathfrak{t}}^{\varsigma(\mathfrak{t})}\nu(\mathfrak{t}) + e^{\nu(\mathfrak{t})} = g(\mathfrak{t}), \tag{36}$$

where

$$g(\mathfrak{t}) = 2\mathfrak{t}^{2-\varrho(\mathfrak{t})}\left(\frac{\Gamma(3-\varrho(\mathfrak{t})) + \Gamma(3-\varsigma(\mathfrak{t}))}{\Gamma(3-\varsigma(\mathfrak{t}))\Gamma(3-\varrho(\mathfrak{t}))}\right) + \frac{\mathfrak{t}^{1-\varrho(\mathfrak{t})}}{\Gamma(2-\varsigma(\mathfrak{t}))} + e^{\mathfrak{t}^2+\mathfrak{t}}, \tag{37}$$

subject to the initial conditions $\nu(0) = \nu'(0) = 0$. The analytic solution in the classical form of this problem is $\nu(\mathfrak{t}) = \mathfrak{t}^2 + \mathfrak{t}$. We implemented the presented approach with $N = 2$ for the approximate solution of this model for $\varrho(\mathfrak{t}) = \dfrac{3}{2}$ and $\varsigma(\mathfrak{t}) = \dfrac{3}{4}$. So, the approximate solution is derived as follows:

$$\nu_2(\mathrm{t}) = 1 \times 10^{-25} + 0.99999999999999999999999996\mathrm{t} + 0.99999999999999999999999994\mathrm{t}^2. \tag{38}$$

Therefore, the numerical solution is equal to the analytical. While, the maximum error reported in [33] by the Bernoulli polynomials with $N = 6$ is $1.02487E-13$. This means that the presented scheme is more efficient and superior with respect to the method of [33] for solving this example.

Example 2. Suppose the Lane–Emden equation in the form

$${}_0^c D_{\mathrm{t}}^{\varrho(\mathrm{t})}\nu(\mathrm{t}) + \frac{2}{\mathrm{t}^{\varrho(\mathrm{t})-\varsigma(\mathrm{t})}}\,{}_0^c D_{\mathrm{t}}^{\varsigma(\mathrm{t})}\nu(\mathrm{t}) - (\nu(\mathrm{t}))^2 = g(\mathrm{t}), \tag{39}$$

where

$$g(\mathrm{t}) = \mathrm{t}^{1-\varrho(\mathrm{t})}\left(\mathbf{E}_{2,2-\varrho(\mathrm{t})}(-\mathrm{t}^2) - \frac{1}{\Gamma(2-\varrho(\mathrm{t}))}\right) + 2\mathrm{t}^{1-\varrho(\mathrm{t})}\mathbf{E}_{2,2-\varsigma(\mathrm{t})}(-\mathrm{t}^2) - \sin(\mathrm{t})^2, \tag{40}$$

in which, we apply the first 20 terms of the Mittag-Leffler series in our computational. The approximation also used in what follows in this paper. The exact solution is $\nu(\mathrm{t}) = \sin(\mathrm{t})$. So, $\nu(0) = 0$ and $\nu'(0) = 1$ are the initial conditions. We apply the proposed technique to compute the numerical solution for this example with different values of N for three selections $\varsigma_1(\mathrm{t}) = 0.8 - 0.1\sin(\mathrm{t})$, $\varsigma_2(\mathrm{t}) = 0.8 - 0.3\sin(\mathrm{t})$ and $\varsigma_3(\mathrm{t}) = 0.8 - 0.5\sin(\mathrm{t})$. Also, three selections $\varrho_1(\mathrm{t}) = 1.8 - 0.35\exp(-\mathrm{t}^2)$, $\varrho_2(\mathrm{t}) = 1.8 - 0.55\exp(-\mathrm{t}^2)$ and $\varrho_3(\mathrm{t}) = 1.8 - 0.75\exp(-\mathrm{t}^2)$ are used.

Table 1: The L_∞ errors in Example 2 with different values of N.

	$\varrho_1(\mathrm{t})$			$\varrho_2(\mathrm{t})$			$\varrho_3(\mathrm{t})$		
N	$\varsigma_1(\mathrm{t})$	$\varsigma_2(\mathrm{t})$	$\varsigma_3(\mathrm{t})$	$\varsigma_1(\mathrm{t})$	$\varsigma_2(\mathrm{t})$	$\varsigma_3(\mathrm{t})$	$\varsigma_1(\mathrm{t})$	$\varsigma_2(\mathrm{t})$	$\varsigma_3(\mathrm{t})$
5	$4.7624E-05$	$4.7416E-05$	$4.7158E-05$	$5.0958E-05$	$5.0910E-05$	$5.0768E-05$	$5.3846E-05$	$5.4017E-05$	$5.4052E-05$
7	$1.7751E-07$	$1.7600E-07$	$1.7447E-07$	$1.9490E-07$	$1.9388E-07$	$1.9257E-07$	$2.1095E-07$	$2.1087E-07$	$2.1074E-07$
9	$3.7149E-10$	$3.6748E-10$	$3.6374E-10$	$4.1514E-10$	$4.1169E-10$	$4.0797E-10$	$4.5710E-10$	$4.5546E-10$	$4.5266E-10$
11	$4.9828E-13$	$4.9226E-13$	$4.8696E-13$	$5.6396E-13$	$5.5812E-13$	$5.5235E-13$	$6.2898E-13$	$6.2516E-13$	$6.2014E-13$
13	$4.6498E-16$	$4.5905E-16$	$4.5403E-16$	$5.3139E-16$	$5.2516E-16$	$5.1934E-16$	$5.9857E-16$	$5.9382E-16$	$5.8832E-16$

Table 1 reports the obtained results for this example. Column one of this table is the number of the $\mathcal{V}t$-$\mathcal{L}$ polynomials (N), which increases from top to bottom and other columns are L_∞ errors between the present method and the exact solution for different values of $\varsigma(\mathrm{t})$ and $\varrho(\mathrm{t})$. With increases in N, one can observe that the error decreases, which indicates the capability of the

present technique. The results of this table show that our scheme is reliable for different values of $\mathcal{V}$-$\mathcal{O}$s.

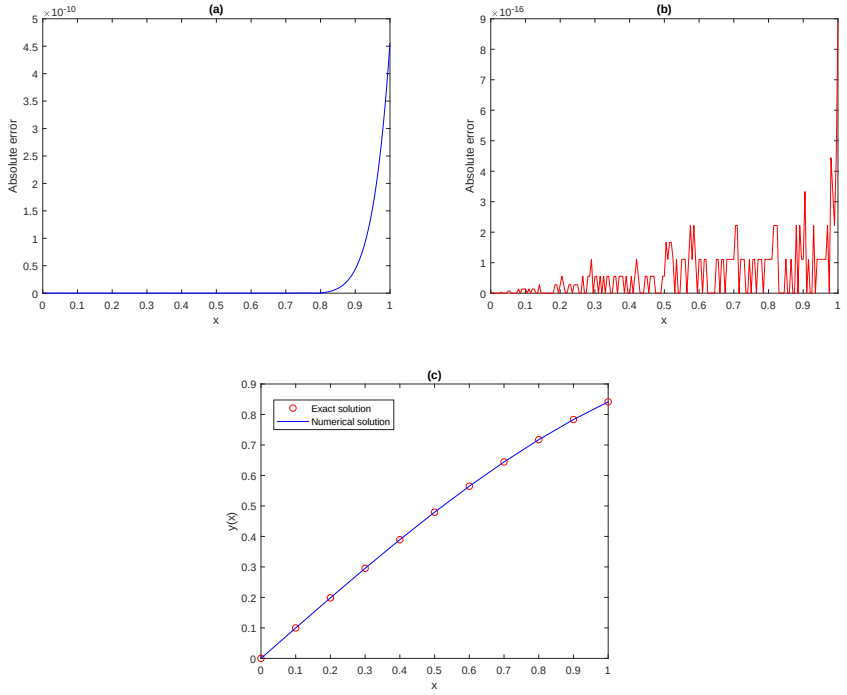

Figure 1: The absolute error of $\nu(\mathfrak{t})$ in Example 2 for $\varsigma_3(\mathfrak{t})$ and $\varrho_3(\mathfrak{t})$ with two values of N, (a) $N = 9$, (b) $N = 13$, and (c) the exact solution and numerical solution $\nu_{11}(\mathfrak{t})$.

Figure 1 (a) and (b) demonstrates the absolute errors for $\varsigma_3(\mathfrak{t})$ and $\varrho_3(\mathfrak{t})$ for different selections of N. Also, Figure 1(c) illustrates the numerical and exact solutions for this problem.

From the results of Table 1 and Figure 1, one can observe that the presented approach is very reliable and capable of calculating the approximate solution of this problem.

Example 3. In this example, we consider the Lane–Emden model as

$$ {}_0^c D_{\mathfrak{t}}^{\varrho(\mathfrak{t})}\nu(\mathfrak{t}) + \frac{4}{\mathfrak{t}^{\varrho(\mathfrak{t})-\varsigma(\mathfrak{t})}}\, {}_0^c D_{\mathfrak{t}}^{\varsigma(\mathfrak{t})}\nu(\mathfrak{t}) + \mathfrak{t}^2\nu(\mathfrak{t}) = g(\mathfrak{t}), \tag{41} $$

subject to the following initial conditions

$$\begin{cases} \nu(0) = 1, \\ \nu'(0) = -1, \end{cases}$$

with

$$\begin{aligned} g(\mathfrak{t}) =& \mathfrak{t}^{-\varrho(\mathfrak{t})}\Big(\mathbf{E}_{1,1-\varrho(\mathfrak{t})}(-\mathfrak{t}) - \frac{1}{\Gamma(1-\varrho(\mathfrak{t}))} + \frac{\mathfrak{t}}{\Gamma(2-\varrho(\mathfrak{t}))}\Big) \\ &+ 4\mathfrak{t}^{-\varrho(\mathfrak{t})}\Big(\mathbf{E}_{1,1-\varsigma(\mathfrak{t})}(-\mathfrak{t}) - \frac{1}{\Gamma(1-\varsigma(\mathfrak{t}))}\Big) + \mathfrak{t}^2\exp(-\mathfrak{t}). \end{aligned} \tag{42}$$

The analytical solution is $\nu(\mathfrak{t}) = \exp(-\mathfrak{t})$. Similar to the previous example, we use the following different selections for the $\mathcal{V}$-$\mathcal{O}$s $\varsigma(\mathfrak{t})$ and $\varrho(\mathfrak{t})$

$$\begin{aligned} &\varsigma_1(\mathfrak{t}) = 0.35 + 0.2\exp(-\mathfrak{t}), && \varsigma_2(\mathfrak{t}) = 0.35 + 0.4\exp(-\mathfrak{t}), \\ &\varsigma_3(\mathfrak{t}) = 0.35 + 0.6\exp(-\mathfrak{t}), && \varrho_1(\mathfrak{t}) = 1.8 - 0.25\cos(\mathfrak{t}), \\ &\varrho_2(\mathfrak{t}) = 1.8 - 0.45\cos(\mathfrak{t}), && \varrho_3(\mathfrak{t}) = 1.8 - 0.65\cos(\mathfrak{t}), \end{aligned}$$

to test our method for approximating the solution of this example.

Table 2: The L_∞ errors in Example 3 with different values of N.

	$\varrho_1(\mathfrak{t})$			$\varrho_2(\mathfrak{t})$			$\varrho_3(\mathfrak{t})$		
N	$\varsigma_1(\mathfrak{t})$	$\varsigma_2(\mathfrak{t})$	$\varsigma_3(\mathfrak{t})$	$\varsigma_1(\mathfrak{t})$	$\varsigma_2(\mathfrak{t})$	$\varsigma_3(\mathfrak{t})$	$\varsigma_1(\mathfrak{t})$	$\varsigma_2(\mathfrak{t})$	$\varsigma_3(\mathfrak{t})$
6	$5.6134E-06$	$5.6705E-06$	$5.6751E-06$	$6.4335E-06$	$6.4244E-06$	$6.3466E-06$	$7.2120E-06$	$7.1085E-06$	$6.9261E-06$
8	$1.4038E-08$	$1.4277E-08$	$1.4400E-08$	$1.6502E-08$	$1.6607E-08$	$1.6531E-08$	$1.9013E-08$	$1.8871E-08$	$1.8493E-08$
10	$2.1893E-11$	$2.2348E-11$	$2.2649E-11$	$2.6141E-11$	$2.6443E-11$	$2.6469E-11$	$3.0683E-11$	$3.0620E-11$	$3.0157E-11$
12	$2.3300E-14$	$2.3834E-14$	$2.4229E-14$	$2.8115E-14$	$2.8541E-14$	$2.8684E-14$	$3.3442E-14$	$3.3513E-14$	$3.3141E-14$
14	$1.7999E-17$	$1.8437E-17$	$1.8778E-17$	$2.1870E-17$	$2.2270E-17$	$2.2457E-17$	$2.6282E-17$	$2.6419E-17$	$2.6210E-17$

The L_∞ errors between the approximate and exact solution are provided in Table 2. The first column of this table is the various values of N from 6 to 14. The next columns are the errors for different selections of $\varsigma(\mathfrak{t})$ and $\varrho(\mathfrak{t})$. It is evident that augmenting the polynomial bases leads to a reduction in error for each $\varsigma(\mathfrak{t})$ and $\varrho(\mathfrak{t})$ value. The convergence of the outcomes presented in this table is readily discernible.

The diagram of the numerical solution and its absolute error is depicted in Figure 2 (a) and (b). Also, the numerical and exact solutions for $\varsigma_3(\mathfrak{t})$ and $\varrho_3(\mathfrak{t})$ are depicted in Figure 2 (c).

Table 2 and Figure 2 confirm that the efficiency of the obtained numerical results is improved by increasing the values of N. These results show the capability of the presented technique for solving this example.

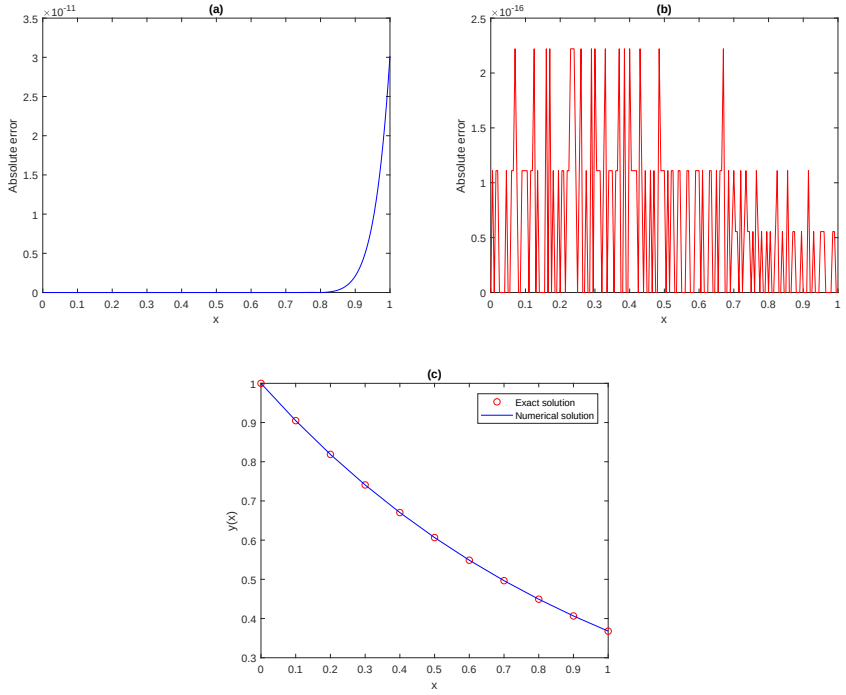

Figure 2: The absolute error of $\nu(\mathfrak{t})$ in Example 3 for $\varsigma_3(\mathfrak{t})$ and $\varrho_3(\mathfrak{t})$ with two values of N (a) $N = 10$, (b) $N = 14$, and (c) the analytical solution and numerical solutions $\nu_{12}(\mathfrak{t})$.

Example 4. In the end, we examine the following Lane–Emden model:

$$\begin{cases} {}_0^c D_{\mathfrak{t}}^{\varrho(\mathfrak{t})}\nu(\mathfrak{t}) + \dfrac{1}{\mathfrak{t}^{\varrho(\mathfrak{t})-\varsigma(\mathfrak{t})}}\,{}_0^c D_{\mathfrak{t}}^{\varsigma(\mathfrak{t})}\nu(\mathfrak{t}) - \dfrac{1}{\mathfrak{t}}\nu(\mathfrak{t}) = g(\mathfrak{t}), \\ \nu(0) = 0, \quad \nu'(0) = 1, \end{cases} \tag{43}$$

where

$$g(\mathfrak{t}) = \mathfrak{t}^{1-\varrho(\mathfrak{t})}\Big(\sum_{i=1}^{\infty}\frac{(2i+1)(-\mathfrak{t}^2)^i}{\Gamma(2i+2-\varrho(\mathfrak{t}))} + \sum_{i=0}^{\infty}\frac{(2i+1)(-\mathfrak{t}^2)^i}{\Gamma(2i+2-\varsigma(\mathfrak{t}))}\Big) + \cos(\mathfrak{t}). \tag{44}$$

The analytic solution is $\nu(\mathfrak{t}) = \mathfrak{t}\cos(\mathfrak{t})$ for any $0 < \varsigma(\mathfrak{t}) < 1$ and $1 < \varrho(\mathfrak{t}) < 2$. We apply the proposed approach for this problem with some different values of $\varsigma(\mathfrak{t})$ and $\varrho(\mathfrak{t})$ as follows:

$$\varsigma_1(\mathfrak{t}) = 0.8 - 0.15\sin(\mathfrak{t})\cos(\mathfrak{t}), \qquad \varsigma_2(\mathfrak{t}) = 0.8 - 0.35\sin(\mathfrak{t})\cos(\mathfrak{t}),$$

$$\varsigma_3(\mathfrak{t}) = 0.8 - 0.55\sin(\mathfrak{t})\cos(\mathfrak{t}), \tag{45}$$

and

$$\varrho_1(\mathfrak{t}) = 0.55 + \frac{1}{1+\mathfrak{t}^2}, \qquad \varrho_2(\mathfrak{t}) = 0.75 + \frac{1}{1+\mathfrak{t}^2}, \qquad \varrho_3(\mathfrak{t}) = 0.95 + \frac{1}{1+\mathfrak{t}^2}. \tag{46}$$

We report the computed numerical results of the proposed scheme for some values of N in Table 3. The results obtained are compiled in Table 3, demonstrating that the outcomes improve as the values of N increase. These findings affirm that the numerical solutions converge toward the analytic solution. Figure 3 (a) and (b) depict the absolute errors for this problem with two values of N. Moreover, the analytical and approximate solutions are depicted in Figure 3 (c). The results of Figure 3 and Table 3 show that the presented technique accurately calculates the approximate solution for this example.

Table 3: The L_∞ errors in Example 4 with different values of N.

	$\varrho_1(\mathfrak{t})$			$\varrho_2(\mathfrak{t})$			$\varrho_3(\mathfrak{t})$		
N	$\varsigma_1(\mathfrak{t})$	$\varsigma_2(\mathfrak{t})$	$\varsigma_3(\mathfrak{t})$	$\varsigma_1(\mathfrak{t})$	$\varsigma_2(\mathfrak{t})$	$\varsigma_3(\mathfrak{t})$	$\varsigma_1(\mathfrak{t})$	$\varsigma_2(\mathfrak{t})$	$\varsigma_3(\mathfrak{t})$
5	$3.3251E-04$	$3.3175E-04$	$3.3075E-04$	$3.0269E-04$	$3.0145E-04$	$3.0018E-04$	$2.7125E-04$	$2.6994E-04$	$2.6870E-04$
7	$1.6665E-06$	$1.6599E-06$	$1.6520E-06$	$1.4679E-06$	$1.4597E-06$	$1.4517E-06$	$1.2746E-06$	$1.2676E-06$	$1.2613E-06$
9	$4.4376E-09$	$4.4146E-09$	$4.3884E-09$	$3.8173E-09$	$3.7928E-09$	$3.7698E-09$	$3.2440E-09$	$3.2257E-09$	$3.2098E-09$
11	$7.2818E-12$	$7.2374E-12$	$7.1886E-12$	$6.1525E-12$	$6.1100E-12$	$6.0712E-12$	$5.1463E-12$	$5.1175E-12$	$5.0931E-12$
13	$8.0775E-15$	$8.0227E-15$	$7.9640E-15$	$6.7287E-15$	$6.6802E-15$	$6.6370E-15$	$5.5596E-15$	$5.5289E-15$	$5.5036E-15$

6 Conclusion

The $\mathcal{V}$-$\mathcal{O}$ fractional in the Caputo form was used to define the $\mathcal{V}$-$\mathcal{O}$ fractional Lane–Emden equation. So, the novelty of the article is the introduction of a novel equation type, which expands the existing knowledge base. The $\mathcal{V}t$-$\mathcal{L}$ polynomials were applied to solve this problem in linear and nonlinear cases. The presented method was based on these polynomials, under which the problem was transformed into an algebraic system of equations. Four examples were considered to show the capability of the obtained results, and they were compared to their analytical solution and the ones obtained by Bernoulli polynomials solutions in the first example. Through this comparison, the advantages and strengths of the constructed method were highlighted, showcasing its superior performance in terms of accuracy. The outcome confirmed

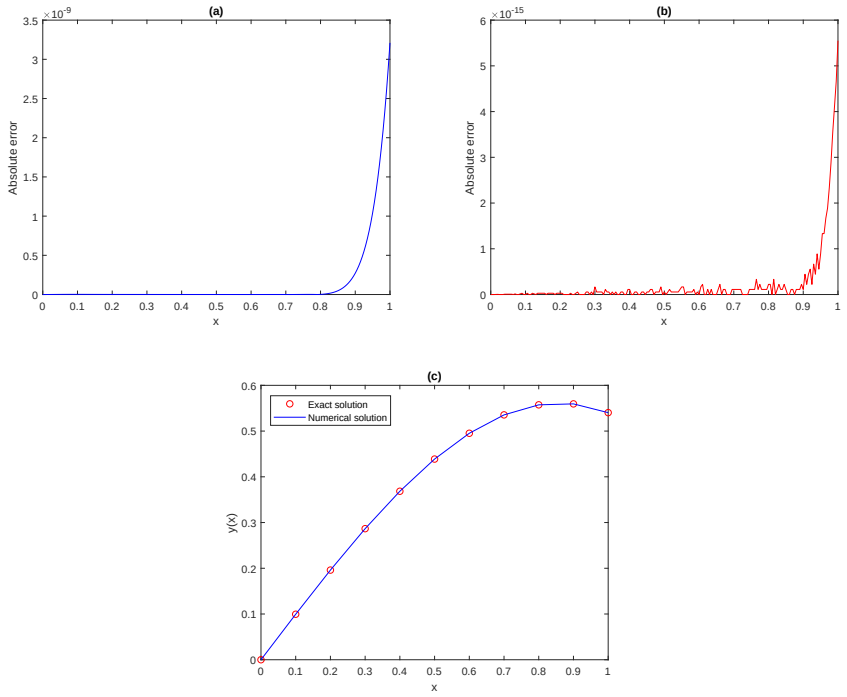

Figure 3: The absolute error of $\nu(t)$ in Example 4 for $\varsigma_3(t)$ and $\varrho_3(t)$ with two values of N (a) $N = 9$, (b) $N = 13$, and (c) the exact solution and numerical solution $\nu_{11}(t)$.

the efficiency and performance of the proposed approach to solve the $\mathcal{V}$-$\mathcal{O}$ fractional Lane–Emden equation. Given the notable precision of $\mathcal{V}t$-$\mathcal{L}$ polynomials in numerically solving the $\mathcal{V}$-$\mathcal{O}$ fractional Lane–Emden equation, future research should focus on several areas: extending the application of this derivative to various other equations and integrating the operator matrix method with other numerical methodologies.

References

[1] Abu Arqub, O., El-Ajou, A., Bataineh, A.S., and Hashim, I. *A representation of the exact solution of generalized Lane–Emden equations using a new analytical method*, In Abstr. Appl. Anal. (Vol. 2013, No. 1, p. 378593), Hindawi, 2013.

[2] Agarwal, P. and El-Sayed, A.A. *Vieta–Lucas polynomials for solving a fractional-order mathematical physics model*, Adv. Diff. Equ. 2020(1) (2020) 1–18.

[3] Bu, W., Tang, Y., Wu, Y. and Yang, J. *Finite difference/finite element method for two-dimensional space and time fractional Bloch–Torrey equations*, J. Comput. Phys. 293 (2015) 264–279.

[4] Caglar, N. and Caglar, H. *B-spline solution of singular boundary value problems*, Appl. Math. Comput. 182(2) (2006) 1509–1513.

[5] Chambré, P.L. *On the solution of the Poisson-Boltzmann equation with application to the theory of thermal explosions*, J. Chem. Phys. 20(11) (1952) 1795–1797.

[6] Chandrasekhar, S. *Eddington: The most distinguished astrophysicist of his time*, Cambridge University Press, 1983.

[7] Choudhury, M.D., Chandra, S., Nag, S., Das, S. and Tarafdar, S. *Forced spreading and rheology of starch gel: Viscoelastic modeling with fractional calculus*, Colloids Surf. A: Physicochem. Eng. Asp. 407 (2012) 64–70.

[8] Coimbra, C.F.M. *Mechanics with variable-order differential operators*, Annal. Phys. 515 (11-12) (2003) 692–703.

[9] Cooper, G.R.J. and Cowan, D.R. *Filtering using variable order vertical derivatives*, Comput. Geosci. 30(5) (2004) 455–459.

[10] Davis, H.T. *Introduction to nonlinear differential and integral equations*, US Government Printing Office, 1961.

[11] Dehghan, M. and Shakeri, F. *Approximate solution of a differential equation arising in astrophysics using the variational iteration method*, New Astron. 13(1) (2008) 53–59.

[12] Flandoli, F. and Tudor, C.A. *Brownian and fractional Brownian stochastic currents via Malliavin calculus*, J. Funct. Anal. 258(1) (2010) 279–306.

[13] Habibirad, A., Hesameddini, E., Heydari, M.H. and Roohi, R. *An efficient meshless method based on the moving Kriging interpolation for two-dimensional variable-order time fractional mobile/immobile advection-diffusion model*, Math. Method. Appl. Sci. 44(4) (2021) 3182–3194.

[14] He, J. H. and Ji, F. Y. *Taylor series solution for Lane–Emden equation,* J. Math. Chem. 57 (2019) 1932–1934.

[15] Heydari, M.H., Avazzadeh, Z. and Razzaghi, M. *Vieta–Lucas polynomials for the coupled nonlinear variable-order fractional Ginzburg–Landau equations*, Appl. Numer. Math. 165 (2021) 442–458.

[16] Heydari, M.H., Avazzadeh, Z. and Yang, Y. *A computational method for solving variable-order fractional nonlinear diffusion-wave equation*, Appl. Math. Comput. 352 (2019) 235–248.

[17] Heydari, M.H., Hooshmandasl, M.R. and Ghaini, F.M.M. *An efficient computational method for solving fractional biharmonic equation*, Comput. Math. Appl. 68(3) (2014) 269–287.

[18] Izadi, M. *A discontinuous finite element approximation to singular Lane–Emden type equations*, Appl. Math. Comput. 401 (2021) 126115.

[19] Izadi, M., Yüzbaşı, Ş. and Ansari, K.J. *Application of Vieta–Lucas series to solve a class of multi-pantograph delay differential equations with singularity*, Symmetry, 13(12) (2021) 2370.

[20] Karimi Dizicheh, A., Salahshour, S., Ahmadian, A. and Baleanu, D. *A novel algorithm based on the Legendre wavelets spectral technique for solving the Lane–Emden equations*, Appl. Numer. Math. 153 (2020) 443–456.

[21] Khalique, C. M. and Muatjetjeja, B. *Lie group classification of the generalized Lane–Emden equation*, Appl. Math. Comput. 210(2) (2009) 405–410.

[22] Kilicman, A., Shokhanda, R. and Goswami, P. *On the solution of (n+1)-dimensional fractional m-burgers equation*, Alex. Eng. J. 60(1) (2021) 1165–1172.

[23] Kumar, M. and Singh, N. *Modified Adomian decomposition method and computer implementation for solving singular boundary value problems arising in various physical problems*, Comput. Chem. Eng. 34(11) (2010) 1750–1760.

[24] Lin, R., Liu, F., Anh, V. and Turner, I. *Stability and convergence of a new explicit finite-difference approximation for the variable-order nonlinear fractional diffusion equation*, Appl. Math. Comput. 212(2) (2009) 435–445.

[25] Magin, R.L., Ingo, C., Colon-Perez, L., Triplett, W. and Mareci, T.H. *Characterization of anomalous diffusion in porous biological tissues using fractional order derivatives and entropy*, Micropor. Mesopor. Mat. 178 (2013) 39–43.

[26] Moghaddam, B.P., Yaghoobi, S. and Machado, J.A.T. *An extended predictor-corrector algorithm for variable-order fractional delay differential equations*, J. Comput. Nonlinear Dyn. 11(6) (2016).

[27] Noor, Z.A., Talib, I., Abdeljawad, T. and Alqudah, M.A. *Numerical study of Caputo fractional-order differential equations by developing new operational matrices of Vieta–Lucas polynomials*, Fract. Fract. 6(2) (2022) 79.

[28] Parand, K., Yousefi, H. and Delkhosh, M. *A numerical approach to solve Lane–Emden type equations by the fractional order of rational Bernoulli functions*, Rom. J. Phys. 62(104) (2017) 1–24.

[29] Patnaik, S., Hollkamp, J.P. and Semperlotti, F. *Applications of variable-order fractional operators: A review,* Proc. R. Soc. A, 476(2234) (2020) 20190498.

[30] Podlubny, I. *Fractional differential equations: an introduction to fractional derivatives, fractional differential equations, to methods of their solution and some of their applications*, Elsevier, 1998.

[31] Robbins, N. *Vieta's triangular array and a related family of polynomials*, Int. J. Math. Math. Sci. 14(2) (1991) 239–244.

[32] Ross, B. and Samko, S. *Fractional integration operator of variable order in the holder spaces hλ (x),* Int. J. Math. Math. Sci. 18(4) (1995) 777–788.

[33] Sahu, P.K. and Mallick, B. *Approximate solution of fractional order Lane–Emden type differential equation by orthonormal Bernoulli's polynomials*, Int. J. Appl. Comput. Math. 5(3) (2019) 1–9.

[34] Samko, S.G. and Ross, B. *Integration and differentiation to a variable fractional order*, Integral Transforms Spec. Funct. 1(4) (1993) 277–300 1993.

[35] Shokhanda, R. and Goswami, P. *Solution of generalized fractional burgers equation with a nonlinear term,* Int. J. Appl. Comput. Math. 8(5) (2022) 1–14.

[36] Shokhanda, R., Goswami, P., He, J.H. and Althobaiti, A. *An approximate solution of the time-fractional two-mode coupled burgers equation*, Fract. Fract. 5(4) (2021) 196.

[37] Singh, R., Das, N. and Kumar, J. *The optimal modified variational iteration method for the Lane–Emden equations with Neumann and Robin boundary conditions*, Eur. Phys. J. Plus, 132 (2017) 1–11.

[38] Sun, H., Chen, W. and Chen, Y.Q. *Variable-order fractional differential operators in anomalous diffusion modeling*, Physica A Stat. Mech. Appl. 388(21) (2009) 4586–4592.

[39] Sweilam, N.H., Nagy, A.M., Assiri, T.A. and Ali, N.Y. *Numerical simulations for variable-order fractional nonlinear delay differential equations*, J. Frac. Calc. Appl. 6(1) (2015) 71–82.

[40] Tseng, C.C. *Design of variable and adaptive fractional order fir differentiators*, Signal Process. 86(10) (2006) 2554–2566.

[41] VanGorder, R.A. *An elegant perturbation solution for the Lane–Emden equation of the second kind*, New Astron. 16(2) (2011) 65–67.

[42] Wazwaz, A.M. and Rach, R. *Comparison of the Adomian decomposition method and the variational iteration method for solving the Lane–Emden equations of the first and second kinds*, Kybernetes, 40(9-10) (2011) 1305–1318.

[43] Xie, L.J., Zhou, C.L. and Song Xu, S. *Solving the systems of equations of Lane–Emden type by differential transform method coupled with Adomian polynomials*, Math. 7(4) (2019) 377.

[44] Zhuang, P., Liu, F., Anh, V. and Turner, I. *Numerical methods for the variable-order fractional advection-diffusion equation with a nonlinear source term*, SIAM J. Numer. Anal. 47(3) (2009) 1760–1781.